Minimizing clogging of geosynthetic drainage – mechanism of erosion of adjacent soil particles

So Takezaki & Kazuto Endo
Center for Material Cycles and Waste Management Research, National Institute for Environmental Studies, Japan

Takeshi Katsumi
Graduate School of Global Environmental Studies, Kyoto University, Japan

ABSTRACT: The mass of internal soil erosion adjacent to a geosynthetic drainage material due to precipitation and percolation was evaluated. Down-flow precipitation/percolation tests using a column diameter of 10 cm and height of 10 cm were conducted on sandy soils under several precipitation intensities. The experimental results showed that there are two patterns which can be differentiated in terms of the masses of soil losses; large soil erosion and small soil erosion. The mass of eroded soils for large soil erosion was approximately 5 times greater than that of small soil erosion. Large soil erosion occurred when sufficient precipitation/percolation intensity for the hydraulic conductivity of soil was continuously given, and is attributed to the seepage failure which occurred when the wetting-front reached the bottom of the column specimen and the condition for all the depth of the specimen reached saturation. In contrast, only preferential flow occurred either with insufficient precipitation/percolation intensity or with a limited period of precipitation with sufficient intensity resulting in small soil erosion. In small soil erosion, the value of the mass of soil erosion from the eroded portions at the bottom of the specimen was up to 90% of the losses. The formation of the eroded portions depends on the falling droplets. A theoretical method to estimate the magnitude of erosion is proposed based on the balance of weight of the droplet and the capillary force. The calculated and measured values of the mass of soil erosion adjacent to the geosynthetic material showed good agreement.

Keywords: Lateral Drainage, Landfill cover, Internal erosion, mass of soil losses, Eroded portion

1 INTRODUCTION

Geosynthetic drainage materials installed in lateral direction in landfill cover systems are expected to provide lateral drainage against percolated water through the overlain cover soil layers. Clogging is an important consideration for the performance of such geosynthetic drainage materials (Giroud et al. 2000, Giroud et al. 2012, Palmeira et al. 2000, Miura et al. 2000, Bell et al. 1980). It is anticipated that clogging may be caused by the intrusion of soil particles into the drainage material, which consequently decreases drainage capacity as illustrated in Figure 1. The internal erosion of the soil particles adjacent to such geosynthetics should be minimized to prevent non-negligible clogging. The evaluation of the permeability of lateral geosynthetic drainage layer using the Kozeny–Carman equation has been proposed (Giroud. 1994). In this approach, the mass of soil losses is necessary to estimate the permeability. However, most previous studies on internal erosion which is considered to govern the soil losses considered only the saturated

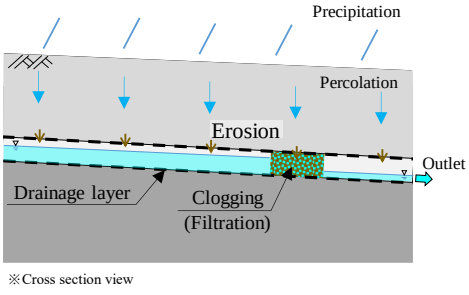

Figure 1. Clogging in drainage layer installed in cover system

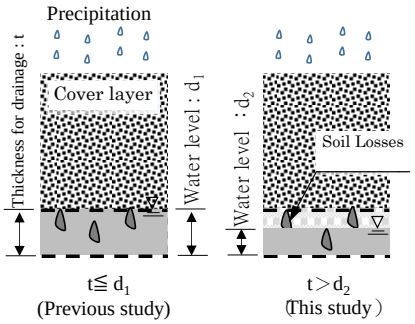

Figure 2. Setting for water level in drainage layer

condition (Ghosh et al. 2004, Hayashi et al 1996), while landfill cover systems consisting of lateral drainage and soil layers are expected in either saturated or unsaturated conditions depending on the hydraulic conditions. On the other hand, The hydraulic head in the lateral drainage layer is necessary to maintain small value in order to reduce the percolation through the low permeability soil layer. Therefore, in this study, the water level should be maintained within the drainage material as illustrated in Figure 2. Limited data is available on the quantitative analysis of such internal erosions. In this study, the mass of internal soil erosion due to precipitation and percolation was quantitatively evaluated. Down-flow column tests were conducted using sandy soil at the optimum water content under several precipitation intensities. Based on the experimental results, influential factors on internal erosion are discussed. The erosion mechanism was hypothesized using uniform arrangement of soil particle diameter and suction, then, a method to estimate the magnitude of soil losses from the upper soil layer was proposed.

2 EXPERIMENTAL PROCEDURE

A permeameter made of PVC column having a diameter of 10 cm and a height of 15 cm, with a stainless steel mesh placed at approximately 5 cm above the bottom, as shown in Figure 3, was used for the experiment. Soil samples at optimum moisture content were filled in 4 layers with a total thickness of 10 cm. Grass-beads were placed at 5-cm thickness at the top of the soil specimen to provide uniform precipitation over the cross section. Silicon grease was coated in advance along the inner side of the column to minimize side-wall leakage. The two soil types used were a mixture of silica sand and clay. The particle size distribution of the soil used is shown in Figure 4; it is categorized as sandy soil based on the Soil Classification System by the Japanese Geotechnical Society (JGS 0051-2009). The physical properties of the soil sample are presented in Table 1. The optimum moisture contents, w_{opt}, were 10.1% (No. 1) and 17.2% (No. 2), and the maximum dry densities, ρ_{dmax}, were 1.930 g/cm^3 (No. 1), 1.587 g/cm^3 (No. 2), respectively, the degree of compaction of the soil specimen for the column test was 70%, and the hydraulic conductivity, k_s, were 7.0×10^{-4} m/s (No. 1) and 2.8×10^{-5} m/s (No. 2). To avoid clogging of the stainless mesh, the opening size of the mesh was set larger than the maximum particle size of the soil used. This provides a conservative condition in terms of erosion, since the geosynthetics will function as proper filtration owing to their smaller openings compared with the stainless mesh used. Down-flow column tests were conducted under several precipitation intensities. Precipitation was supplied by waterdrops of tap water from 4 injection needles located above the column. The frequency of waterdrops (rainfall intensity) was controlled by hydraulic heads. The effluent was collected by the bottle placed below the column. The elapsed time zero of this test was set at the time of the beginning of outflow. At each interval (depending on precipitation intensities), the total mass of the effluent was measured, and then was subjected to oven-drying to determine the mass of soil particles eroded by precipitation and percolation. For the selected experimental cases, the water contents of the soils at 3 and 9 cm above the bottom of the soil column were

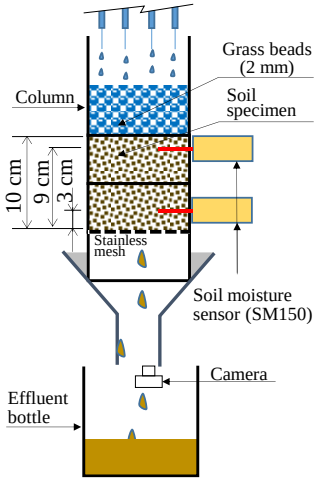

Figure 3. Test apparatus

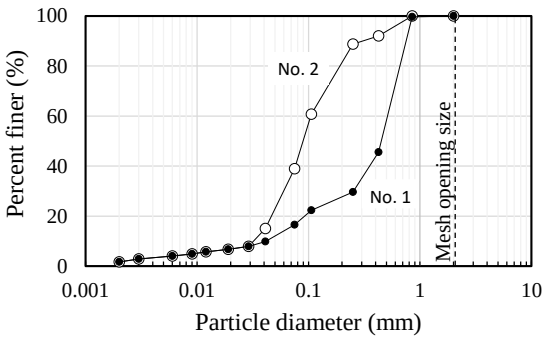

Figure 4. Particle size distribution of the soils used

Table 1. Soil properties

Item	Value	
	No.1	No.2
Soil particle density	2.633 g/cm^3	2.625 g/cm^3
Maximum dry density	1.930 g/cm^3	1.587 g/cm^3
Optimum moisture content	10.1%	17.2%
Porosity at column test	48.7%	57.7%

also measured with time using soil moisture sensors (Delta-T Devices, SM-150). Visual observations below the stainless mesh were carried out from the lower part of the experimental setup.

3 EXPERIMENTAL RESULTS ON INTERNAL EROSION

The cumulative soil losses with precipitation for two types of specimens are shown in Figure 5 for the case of several precipitation intensities, as an example. The soil losses of all cases increased in the first measurement, then gradually increased. The soil losses in first 60 min corresponded to 90% of the total soil losses in this test. Most of the soil particle losses occurred at the beginning of outflow from specimen. Therefore, evaluating the soil losses in the initial stage is important for the estimation of total soil losses. The relationship between the mass of soil losses and precipitation intensities are shown in Figure 6. In this figure, the *x*-axis is the normalized rainfall intensity (NRI), which is defined as the ratio of the precipitation intensity to the seepage velocity based on Darcy's law at a unit hydraulic gradient (i = 1). The *y*-axis values are the masses of soil losses per unit area (1 cm^2) per 100 mL percolation. Only the mass of soil losses at the initial stage, but not the total period, were considered in this graph. Regarding specimen No. 1, only 0.002 g/cm^2 soil losses were observed when the NRI was lower than 8.0%, while for NRI

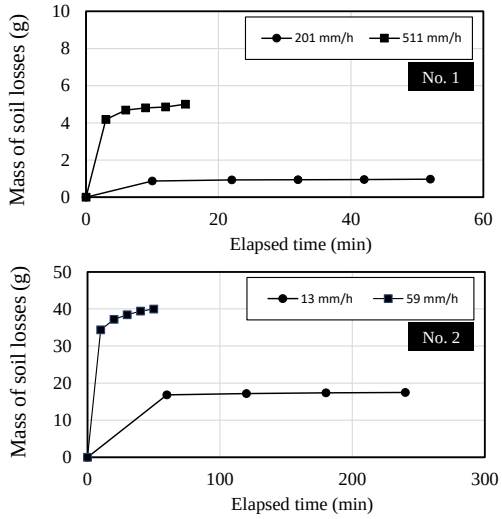

Figure 5. Mass of soil losses

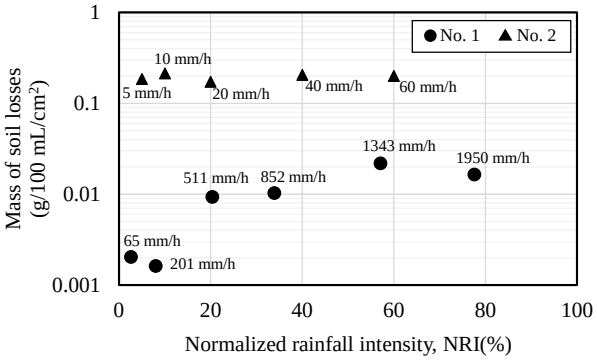

Figure 6. Relationship between precipitation and masses of soil losses

values higher than 20%, significantly higher soil losses of approximately 0.01 g/cm^2 were observed. For specimen No. 2, 0.2 g/cm^2 monotonous soil losses were observed for all ranges of the NRI in this test. Experimental results of the soil losses can be classified into two patterns; large soil erosion and small soil erosion. The temporal behavior of the percolation over the soil depth is an important consideration for the soil erosion. To evaluate the percolation over the specimen, volumetric the moisture contents of the soil samples at 3 and 9 cm above the bottom of the column were measured using soil moisture sensors for 10% and 27% NRI for specimen No. 1, which are below and over the considerable threshold values of the NRI (8–20%) respectively, between large soil erosion and small soil erosion. The experimental results are shown in Figure 7. For the case of the NRI of 10%, the volumetric moisture content at 3 cm height increased faster than at 9 cm, and different moisture contents were observed even when steady the state condition was achieved after approximately 700 s; at the end of experiment, a differential moisture content was maintained. For the case of the NRI of 27%, the volumetric moisture content at 9 cm height increased faster than at 3 cm, and uniform moisture contents were indicated at all depths of the specimen, which suggests that the wetting-front exists and moved downward. The threshold value between large soil losses (erosion) and small soil losses (erosion) may fall between 8% and 20% of the NRI. The masses of losses, as well as visual observations of the soil erosion were clearly different for large soil erosion and small soil erosion as shown in Figure 8, which shows photographs of the bottom of the soil specimens. For small soil erosion cases, few eroded portions with limited soil erosions were observed and yielded muddy water, while cases of large soil erosion caved the entire of bottom.

Schematic diagrams for two patterns of soil erosion are shown in Figure 9. In the pattern for small soil erosion, the formation of the saturated area occurred at the bottom of the specimen. The load of the hydraulic pressure on the bottom of the specimen indicated a small value owing to the relation between the suction and weight of water; therefore, the mass of soil losses was negligible because the number of eroded portions are limited. On the other hand, in the pattern for large soil erosion, the generation of suction did not exist because the entire depth of the specimen was ultimately in a saturated condition. Consequently, the load of the hydraulic pressure at the bottom of the specimen indicated a value 1corresponding to the height of the specimen; a proportional relationship exists between the height of the specimen and the mass of soil losses as illustrated in Figure 10. The mass of soil losses was maximum because the formation of the eroded portions were not limited. The large soil erosion is attributed to the seepage failure which occurred when the wetting-front reached the bottom of the column. These results suggest that the wetting-front should not reach the bottom of the column to avoid large soil erosion.

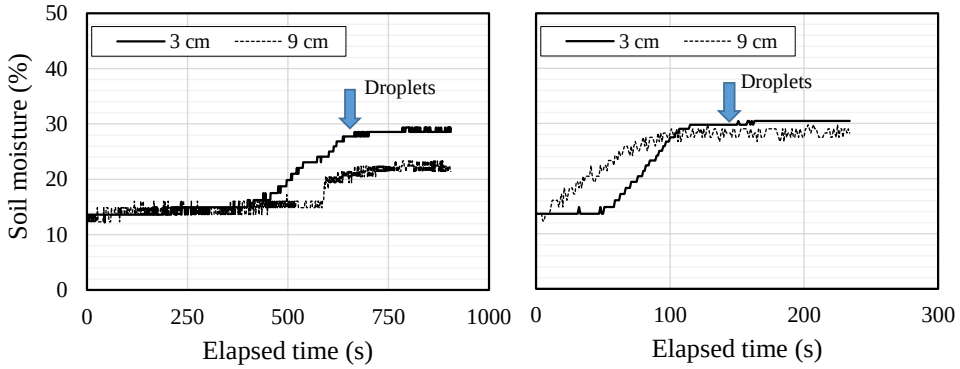

(a) Precipitation intensity 250 mm/h (NRI 10%) (b) Precipitation intensity 690 mm/h (NRI 27%)

Figure 7. Soil moisture with time in the specimen

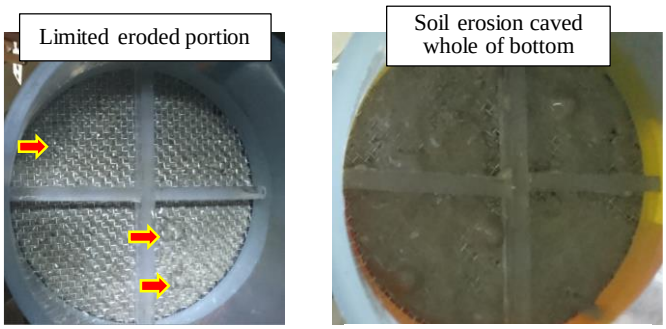

Figure 8. Conditions at the bottom of soil specimen

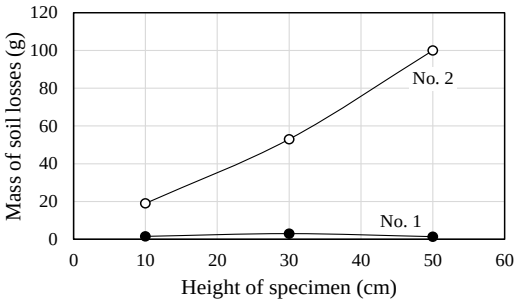

Figure 10. Relation between height of speicmen and mass of soil losses

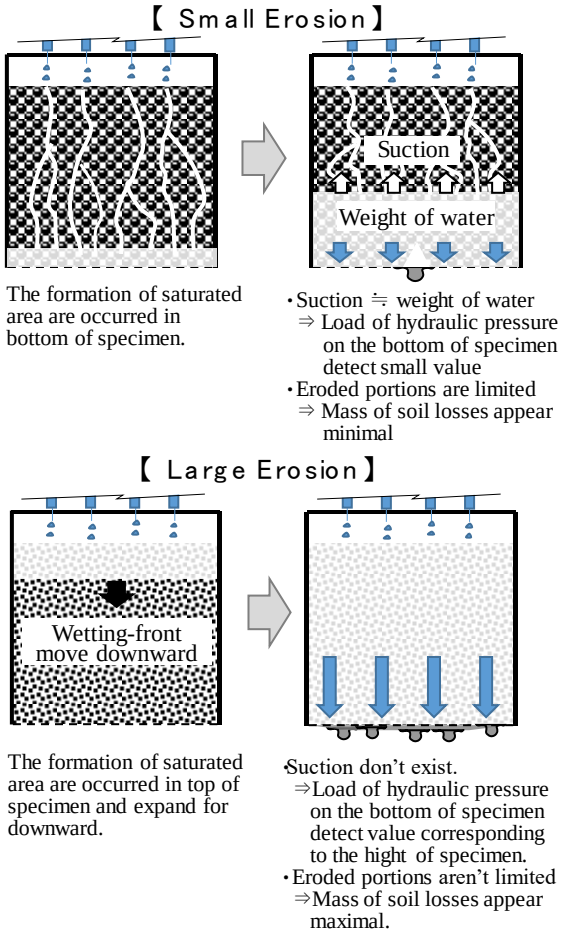

Figure 9. Schmatic diagram for two patterns of soil erosion

4 ESTIMATION OF MASS OF SOIL LOSSES DUE TO FALLING DROPLETS

The above experimental results showed that there are two patterns of soil erosion depending on the conditions: large soil erosion and small soil erosion. In a practical design, the situation caused by large soil erosion can be avoided by selecting suitable materials as cover soil. However, even in the case of the design condition for avoiding large soil erosion, a small amount of soil erosion can occur, and there will still be the concern that the accumulation of eroded soil particles may result in clogging. Therefore, evaluating the soil erosion properties at the conditions of small soil erosion is necessary.

4.1 *Influential factor for mass of soil losses*

Figure 11 shows the mass of soil losses per one eroded portion. The masses of soil losses per one eroded portion were identical, while the total soil losses varied depending on the precipitation intensity. Therefore, it is reasonable to hypothesize that the unit eroded portion involves a mass of soil losses. The estimation of total mass of soil losses is considered to multiply the mass of soil losses per eroded portion and the number of portions together. Visual observations and inspections, which were carried out at the bottom of soil specimen for the case of small soil erosion, showed that soil losses were induced by "droplets" which were originally retained with the soils, but finally fell off. The fallen droplets contained water and soil particles. The size of the droplet did not change while the area of the eroded portion was gradually increased to finally achieve a similar size of the droplet as shown in Figure 12. These states suggest that the droplet size provided a maximum size of the eroded portion and consequently an influential mass of soil losses per eroded portion. Estimating the droplet size and the number per area is expected to provide the prediction of total soil losses over a unit area, particularly in the early stage of the precipitation.

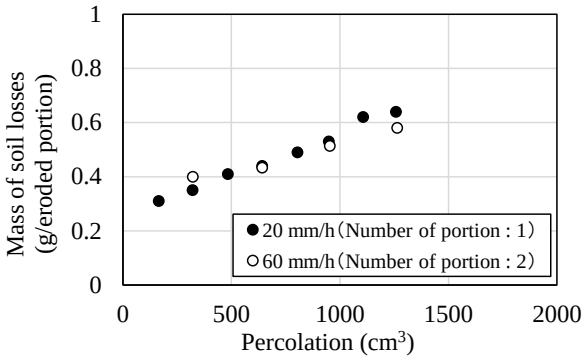

Figure 11. Mass of soil losses per eroded portion at the beginning period of precipitation

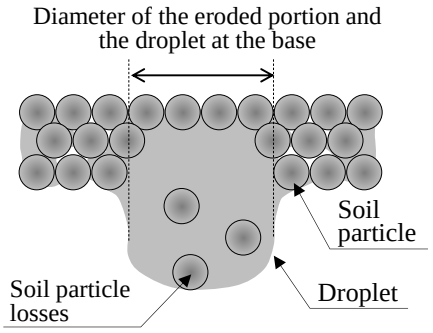

Figure 12. Relation between the droplet and size of eroded portion

4.2 *Balance of forces on the droplet*

The droplet size (or weight) is estimated in this subsection. The two forces acting on the droplet, namely the capillary pressure and droplet weight, are assumed to be balanced as illustrated in Figure 13. If the droplet weight exceeds the capillary force, the droplet will not be retained and will fall off from the soil specimen. However, the capillary pressure is related to the formation of droplet supplied by the force, spots for occurrence of force does not locate at just the individual soil particles but also the mass of soil particle. Therefore, a typical diameter of the particle and the capillary pressure per one void with a schematic for the particle model and water retention characteristics should be developed, as shown in Figure 14. The capillary pressure can be estimated using the number of voids between particles and the value of the capillary pressure per one void can be expressed as follows:

$$F_m = \left(\frac{L_m}{2r}\right) \times \left(\frac{L_m}{1.73r} - 2\right) \times 2 \times f_s \quad (1)$$

where F_m is the the capillary pressure in the model (Pa), L_m is the side length (m), r is a typical radius of the particle (m), and f_s is the capillary force per one void (Pa). Then, the relation between the estimated capillary force from this model and the measured capillary force is considered using Equation (2).

$$\left(\frac{L}{2r}\right) \times \left(\frac{L}{1.73r} - 2\right) \times 2 \times f_s = F_d' \tag{2}$$

1where F_d' is the capillary pressure at the beginning of the drainage in water retention characteristics (Pa). Next, the relation between the capillary force per one void and typical radius of the particle can be expressed as follows:

$$f_s = 2\pi \times \sqrt{\frac{3.46r^3 - 0.67\pi r^3}{2r} \times \frac{1}{\pi}} \times T\cos\theta \tag{3}$$

where, T is the surface tension (72.75 mN/m), and θ is the angle of contact (0). Then, the capillary force per one spot and typical size of the particle are estimated using Equations (2) and (3) and the capillary pressure at the beginning of the drainage, F_d'. For instance, to estimate the values for the condition, L = 1 m and F_d' = 1 cm ($\fallingdotseq$ 0.1 kPa = 0.1 kN/m^2), we obtain that the capillary force per one void, f_s = 2.6 $\times 10^{-4}$ N/void, and a typical size of the particle, r = 1.2 $\times 10^{-3}$ m.

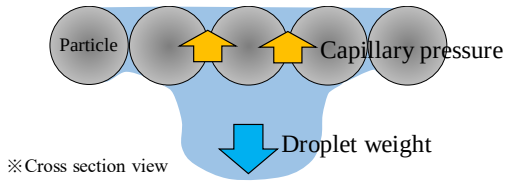

Figure 13. Relationship between the droplet and capillary force

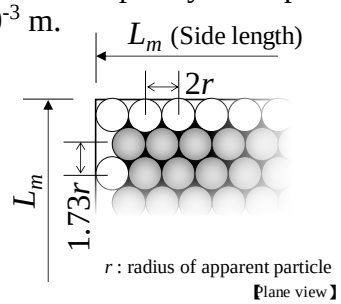

Figure 14. Distance between two lines for center of soil particle in staggered arrangement

4.3 *Comparison between estimated and measured weight of droplet*

The area for the formation of the droplet is assumed to be a square with length of a side, L_d. The capillary force for the entire area can be expressed using Equation (4) as follows:

$$F_d = \left(\frac{L_d}{2r}\right) \times \left(\frac{L_d}{1.73r} - 2\right) \times 2 \times f_s \tag{4}$$

where F_d if the capillary pressure in the area for the formation of the droplet (Pa), and L_d is the length of a side of a square (m). The weight of the droplet is evaluated using the radius of the base of the equivalent circle for the square with length of a side, L_d, which can be expressed as follows (Nakajima. 2007):

$$r_w = \sqrt[3]{3 \times I^2 \times (r_d \div 2)} \tag{5}$$

$$W_w = \frac{4}{3} \times \pi \times r_w^3 \times \rho_w \times g \tag{6}$$

where r_w is the radius of the droplet, I is the capillary length (0.2×10^{-3} m (Nakajima. 2007)), r_d is the radius of the equivalent circle of the square of a side, L_d (m), W_w is the droplet weight (mN), ρ_w is density of water (kg/m^3), and g is gravitational acceleration (m/s^2). The relation between the capillary force and droplet weight can be established using Equations (4), (5), and (6). The estimation result with varying length of a side of a square is shown in Figure 15; the capillary force is smaller than the droplet weight when the length of a side of the square is small, which indicates that the droplet was not retained by capillary and fell off from the soil specimen. When the capillary force and droplet weight are equal, the droplet begins to fall. In this calculation, the condition that the capillary pressure at the beginning of the drainage in water retention characteristics F_d is 0.4 cm providing the above situation was 17 mm for of a side of the square and 2.4 mN for the estimated droplet weight. Experimental results using specimen No. 1 showed that the weight of the droplet was approximately 2.4 mN. Since this value is very close to the value obtained from the above theoretical calculation, the hypothesis to explain the development of

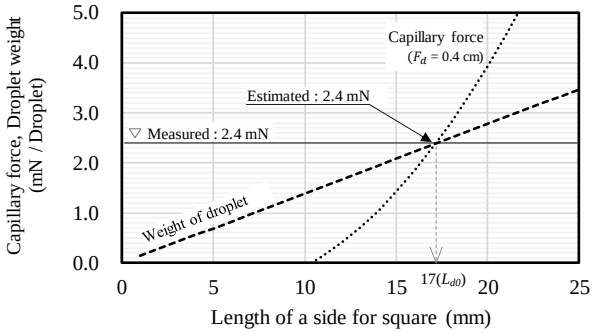

Figure 15. Relationship between the droplet weight and capillary force (measured, estimated)

a droplet is verified. However, estimating the value of the capillary pressure at the beginning of the drainage F_d' is required small range below the value of 1 cm.

4.4 *Evaluation of total mass of soil losses*

The total mass of soil losses is considered to estimate the value of losses multiplied by the mass of soil losses per eroded portion and number of portions together. The radius size of the eroded portion is meant at the base for formation of droplet is considered using Equation (7) and the calculated weight of the droplet.

$$R_p = \sqrt{(L_{d0})^2 \div \pi} \tag{7}$$

where R_p is the radius of the eroded portion and L_{d0} is the estimated value for length of side for square at the droplet falling (for instance, using Figure. 15), Here, calculated value of diameter for portion using Equation (7), with the length 17 mm (Figure 15) will indicate 19mm. That value is similar measurement one as shown in figure 16, the hypothesis to evaluate the portion size have been proven. On the other hand, the number of eroded portions will be evaluated with the volume of percolation and the area of one eroded portion because spots of flow-out of the percolation will be restricted to the eroded portions. The number of portions can be expressed as follows:

$$N = \frac{I \times A}{\pi \times R_p^2 \times (k_0 \times i \times \alpha_p)} \tag{8}$$

where N is the number of eroded portions, I is the rainfall intensity (m/h), A is the area of investigation (m^2), k_0 is the unsaturated hydraulic conductivity (m/s), i is the hydraulic gradient (1) and α_p is the hypothesis coefficient. Figure 17 shows the comparison the number of eroded portions between estimated and measured in case of several rainfall intensity. Increase in number of potions was followed with multiplication of rainfall intensity. Then, hypothesis coefficient α_p was set 0.40, the number of portions estimated by round up processing and measured were showed identical value under almost all cases of rainfall intensity, the formula (8) to explain the number of the eroded portions is verified. Then, the total mass of soil erosion is obtained using the number of the eroded portions and the radius of the eroded portion, R_p, as follows:

$$M = \frac{4}{3}\pi R_p^3 \times N \times \rho_d \times \alpha_s \tag{9}$$

where M is the total mass of soil erosion (g), ρ_d is the dry density of the specimen (g/cm^3) and α_s is the hypothesis coefficient of shape for eroded potion. The total mass of erosion was calculated using Equation (9). The experiment was also conducted using specimen No. 1. These results are shown in Figure 18. From Figure 18, the calculated and measured values of the total mass of soil losses showed good agreement under several rainfall intensities with hypothesis coefficient α_s was set 0.50. The application of this hypothesis is considered to be beneficial to explain soil losses due to internal erosion.

5 EFFECT OF FILTER OPENING SIZE ON SOIL LOSSES

The influence of soil losses should be considered to evaluate the value of soil losses due to differential opening sizes of filter of the drain material surface. Therefore, the mass of soil losses was checked using several opening sizes of the stainless mesh located below the specimen. These results are presented in Table 2. The relation between a smaller opening size of filter-mesh and a reduction in the value of soil losses was out of proportion. The smallest soil losses was occurred at a mesh opening size 0.67 mm, but which opening size was not minimum. This result suggest that the optimum condition for the opening size will exist to reduce the mass of soil losses. The behavior under filtration can depend on the particle size of the soil; in this study, a typical size of the soil particle will adopt the value of d_{85} in the particle size distribution of the soil (Mitchell. 1986). Particle size d_{85} of specimen No. 1 was 0.73 mm, and the opening size that reduced soil losses was 0.67 mm, the two sizes are similar. On the other hand, the weight of losses at least 64% was considered to be clogging the mesh using an opening size of 0.32 mm, and in this condition, it is difficult for outflow to pass through the clogging mesh below the eroded portion. Therefore, the eroded portion will expand to secure the percolation passing area on the mesh (Mitchell. 1986). For this reason, it is considered that the value of soil losses with 0.32 mm mesh was more than that value with 0.67 mm mesh. These results suggest that a reduction in soil losses will be possible by adjusting the filter mesh opening size to a particle size d_{85} of the specimen.

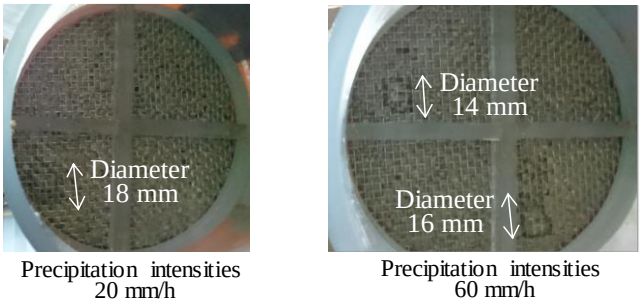

Figure 16. Size of portion (measurement)

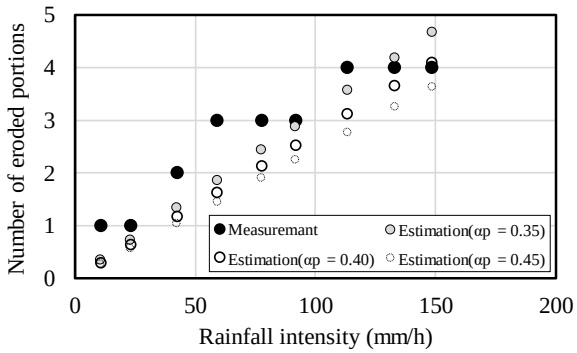

Figure 17. Relation between measured and estimated number of eroded portions

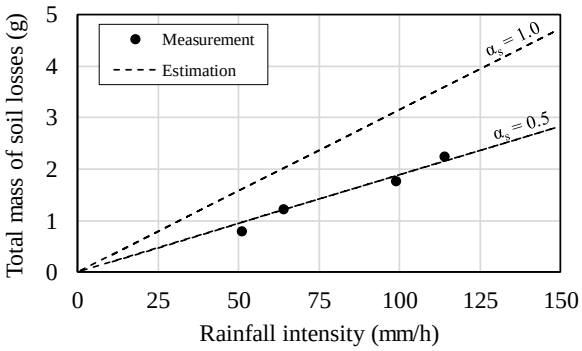

Figure 18. Relation between measured and estimated total mass of soil losses

Table 2. Relation between opening size of filter

Opening size of filter (mm)	Mass of soil losses (g/100 mL/cm^2)
2.19	1.6×10^{-3}
0.67	4.4×10^{-4}
0.32	7.3×10^{-4}

6 CONCLUSIONS

Internal soil erosion adjacent to geosynthetic drainage material due to precipitation and percolation was evaluated. Down-flow precipitation/percolation tests using a column with a diameter of 10 cm and height of 10 cm were conducted on sandy soil for several precipitation intensities. Furthermore, theoretical discussions on how the water droplet was developed at the bottom of the soil particles were presented. The main conclusions from the study are summarized below.

1) Most of the soil particle losses were generated in the early period of precipitation from the precipitation/percolation column tests.
2) There were two patterns which can be differentiated in terms of the masses of soil losses: large soil losses (erosion) and small soil losses (erosion).
3) The depth of the wetting-front and the condition for all depths of the specimen reached were influential factors of internal erosion for large soil losses.
4) The masses of soil losses per eroded portion had almost the same value in different precipitation intensity for small soil losses. A theoretical method to estimate the size of the erosion with the droplet size was proposed based on the balance of the weight of the droplet and the capillary force.
5) To estimate total mass of soil losses, the value of losses was multiplied by the mass of soil losses per eroded portion and the number of portions. The calculated values using the proposed method and the measured values of the total mass of soil losses showed good agreement under several rainfall intensities.
6) The relation between a small opening size of the filter-mesh and reduction in the value of soil losses was out of proportion. Owing to this, the eroded portion will expand to secure the percolation passing area on the mesh, therefore, the eroded portion will expand to secure the percolation passing area on the mesh.

ACKNOWLEDGMENTS

This work was supported by the Nohmura Foundation for Membrane Structure’s Technology.

REFERENCES

Bell, J. R., Hicks, R. G. (1980). Evaluation of test method and use criteria for geotechnical fabrics in highway applications. Interim report no. FHWA/RD–80/021, Federal Highway Administration.

Ghosh, C., Yasuhara, K. (2004). Clogging and flow characteristics of a geosynthetic drain confined in soils undergoing consolidation. Geosynthetics International, Vol. 11, No. 1, pp. 19–34.

Giroud, J. P. (1994). Quantification of Geosynthetic Behavior. Proceedings of the Fifth International Conference on Geotextiles, Geomembranes and Related Products, Vol. 4, pp. 1249–1274.

Giroud, J. P., Gourc, J. P., Kavazanjian, E. Jr. (2012). Laminar and non-laminar flow in geosynthetic and granular drains. Geosynthetics International, Vol. 19, No. 2, pp. 160–182.

Giroud, J. P., Zornberg, J. G., Beech, J. F. (2000). Hydraulic design of geosynthetic and granular liquid collection layers comprising two different slopes. Geosynthetics International, Vol. 7, Nos. 4–6, pp. 453–489.

Hayashi, H., Mori, A. (1996). One proposal on the design of nonwoven geotextile filter layer considering permeability due to clogging. Journal of Japan Society of Civil Engineers, No. 553, No. VI33, pp. 155–170 (in Japanese).

Mitchell, J. K. (1986). Practical problems from surprising soil behavior (The 20th Karl Terzaghi Lecture). J. Geotechnical Engineering, ASCE, Vol. 112, No. 3, pp. 150–161.

Miura, N., Chai, J. C. (2000). Discharge capacity of prefabricated vertical drains confined in clay. Geosynthetics International, Vol. 7, No. 2, pp. 119–135.

Nakajima, A. (2007). Principles of Water and Surface Mechanics. Uchida Rokakuho Publishing, pp. 53–58 (in Japanese).

Sherard, J. L., Dunnigan, L. P. (1989). Critical Filters for Impervious Soils. Journal of geotechnical Engineering, Vol. 115, No. 7, pp. 684–700.